ICOCEM
4. International Conference on
Civil and Environmental
Geology and Mining Engineering
Trabzon - TURKEY
20 - 22 APRIL 2019

Geoelectrical Prospecting For Deep Fracture Aquifers in Kadna, Part of Minna Sheet164 SW, North Central Nigeria

Christopher Imoukhai UNUEVHO[1*], O. Johnson AJIROBA[2], A. Nnosike AMADI[1], K. Mosto ONUOHA[3], E. Emeka UDENSI[4]

[1] Department of Geology, Federal University of Technology, Minna, Nigeria
[2] Kwara State's Ministry of Industry and Solid Minerals Development, Ilorin, Nigeria
[3] Department of Geology, University of Nigeria, Nsukka
[4] Department of Physics, Federal University of Technology, Minna, Nigeria

*Corresponding Author: unuevho@gmail.com

Abstract

Kadna is an urban sprawl of Minna in North-Central Nigeria. It is populated largely by middle class civil servants that obtain fresh water from six boreholes which produce from shallow fractures. The boreholes are now inadequate to satisfy the water requirements of the spiraling population. Opportunity for increasing the fresh water supply lies in exploiting fractures within depths greater than 60 m. The search for groundwater convergence areas within these deep fractures in Kadna was conducted using surface geological mapping and geoelectrical sounding. *Rockwork* was employed to plot Rosette diagram of measured joint directions. SAS 4000 ABEM terrameter was employed to conduct 1D-geoelectrical sounding comprising electrical resistivity, spontaneous potential (SP) and induced polarization (IP) within traverses oriented along foliation strike. The resistivity sounding data was processed and analysed using *WinResist* inversion software, while the SP and IP were plotted and analysed using *Microsoft Excel*. The modeled resistivity sounding curves revealed deep fractures of the HKH, HKHK, HKHKH and KHKHKH curve types. They are confined fractures characterised by 60 – 313 Ωm resistivity, SP values of -75 to +75 mv, basal elevation of 120 – 220 m, (with respect to sea level) and IP values of 10 – 200 ms. Groundwater convergence area was inferred within the deep fractures in the easternmost part, within longitude E6.596° to E6.610° and latitude N9.561° to N9.566°. This is the choicest area for water borehole drilling, being characterised by 100 - 200 Ωm electrical resistivity, -30 to +50 mv spontaneous potential, basal elevation lower than 180 m, and 10 – 13.3 m fracture thickness. The second ranking choice area for drilling lies within longitude E6.5945° to E6.5965° and latitude N9.561° to N9.566°. The third ranking choice area for drilling lies within longitude E6.5945° to E6.5965° and latitude N9.561° to N9.566°.

Keywords: Fresh water, Geoelectrical sounding, Deep fractures, Groundwater convergence

Introduction

Kadna is a satellite suburb of Minna within the part of Nigerian Basement Complex called Northern Nigerian Massif. Its geographical location is defined by latitudes N9°33'30" to N9°34'30" and longitudes E6°32'30" to E6°36'30" (Figure 1).

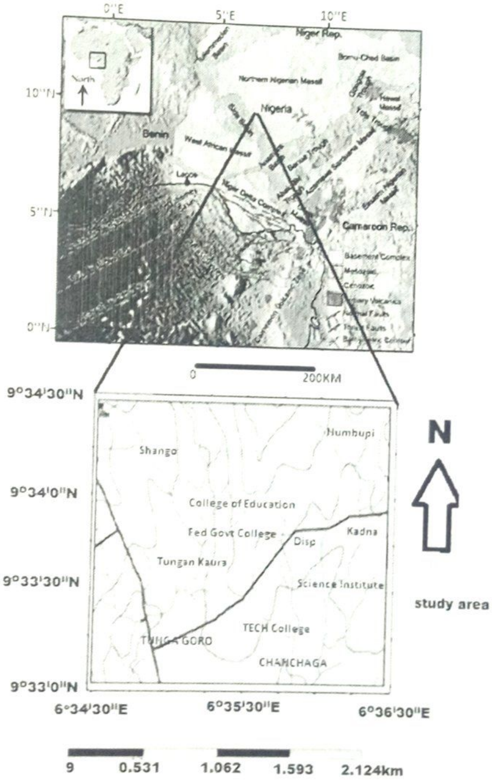

Figure 1. Location of Kadna

The town provides home for workers of Federal Government College, Federal Government Science Equipment Development Institute, Niger State College of Education and Niger State Technical College. The inhabitants outside the Federal Government College premises obtain fresh water presently from only six boreholes. The boreholes are hand-pumped, and thus tap water from fractures shallower than 60m depth. Soaring population has rendered these boreholes inadequate to meet the inhabitants fresh water needs. A plausible approach to providing adequate fresh water lies in exploiting deeper fractures. The search for deep water-bearing fractures requires holistic interpretation of geological and multi geoelectrical data. Such work is yet to be conducted over the entire Kadna town.

Four major petro-litholoical units distinguishable in the Nigerian Basement Complex are Migmatite-Gneiss Complex, the Schist Belts, Older Granites, and undeformed acid and basic dykes. The schist belts consist of pelites, semi-pelites, quarzites, marble, banded iron formation, amphibolites, and minor felsic to intermediate metavolcanic rocks. Oluyide (1988) analysed structural trends in the Nigerian Basement Complex. He found that fractures constitute a major characteristic feature of the complex. He concluded that the principal trends of the fractures are N-S, NNE-SSW, NE-SW, NNW-SSE and NW-SE. He also reported minor E-W fractures. Ajibade et al. (2008) recognized fracture zones within fresh rocks as basement aquifers. They remarked that the fractures are often shallow, and boreholes are commonly 30-40 m deep but occasionally up to 50 m depth in basement areas. Olorunfemi (2009) and Ojo and Olorunfemi (2013) recognized unconfined fractures and confined fractures. They identified a confined fracture as a fractured basement column that is sandwiched between fresh basement above and below.

Direct current(DC) resistivity method is widely employed to generate prospects for drilling productive boreholes in the basement complex (Ayuk et al., 2014; Ojoina, 2014; Wright, 2015) because DC resistivity method is the most suitable among all geophysical methods for delineating aquifers in hard rock terrains (Ratnakumari et al., 2012). However, Tswako et al. (2017) revealed that drilling success rate will be improved by holistic interpretation of resistivity, spontaneous potential (SP) and induced polarization (IP) data to delineate groundwater convergence areas. Dan-Hassan (1999) and Unuevho et al. (2016) highlighted that boreholes are commonly productive within groundwater convergence zones in the Nigerian Basement Complex.

This work seeks to delineate groundwater convergence zone within deep fractures within Kundu, where there is high potential for water boreholes to be productive.

Material and Method

Surface geological mapping was conducted to ascertain the outcropping rock types, the strike as well as dip direction and dip magnitude of the exposed foliated rocks. Fresh samples of rock outcrops were taken for lithology identification during the mapping. Texture and mafic colour index(MCI) were employed to identify the outcrop lithologies. The MCI represents the percentage of mafic (green, dark gray and black) minerals in the rock. Non-foliated rocks with 0-15% MCI were identified to be felsic rocks. Felsic rocks with higher potassium feldspar (pale orange to pink colour) than plagioclase feldspar (light gray in colour) were recognized as granite. Light to gray rocks with schistose texture were identified to be schists. Rocks with glossy minerals characterised by $60^{\circ}/120^{\circ}$ intersecting cleavage planes were called amphibolites. Rocks with mixed gneissic and granitic textures were grouped as migmatites. Non-foliated rocks composed solely of fused buff to white quartz were named quarzites. The locations of the outcrops were plotted on a base map of scale 1: 10,000 produced from Minna Topograhic Sheet 164 SW of scale 1: 50,000. The geologic map of the mapped area was produced from the base map with outcrop locations. Joint directions were measured and the principal joint directions were captured from Rosette plot of the directions, using *Rock Work*. One- dimensional (1D) geoelectrical sounding – comprising resistivity, spontaneous potential (SP) and induced polarization (IP) – was conducted at 50 stations, using Schlumberger array along a traverse of 200 m maximum electrode spacing. The sounding was performed using SAS 4000 ABEM Terrameter, along 10 traverses oriented along foliation strike, with an average of 5 stations per traverse. The traverses were separated by 50 – 100 m along foliation dip direction. Geographic coordinates of the sounding stations were determined using global positioning system (GPS, the etrex Garmin-legend type). The electrical resistivity data were analysed using *WinResist* inversion software. The IP and SP curves were plotted using *Microsoft Excel* and then analysed.

Fracture intervals were identified from the 1D resistivity inverse models. Fractures deeper than 60 m were grouped together as deep fractures. The depth to the base of each deep fracture interval was subtracted from the corresponding sounding station's surface elevation.

This gives the basal elevation of the fracture's interval with respect to sea level. The deep fracture interval thickness was obtained as the difference in depth to top and base of the interval. Iso resistivity, IP and SP maps were generated by contouring the respective parameters against the stations' geographic coordinates. Fracture thickness and basal elevation maps were also generated. Topographic depressions were identified on the basal elevation map. Topographic depressions characterized by low resistivity and increasing SP positivity were inferred to be groundwater convergence zones.

Research Findings and Discussion

The surface lithologic mapping revealed outcrops of migmatite (Figure 2), schist (Figure 3), amphibolite (Figure 4), quartzite (Figure 5) and granite (Figure 6) in the area. The schist and amphibolites bodies strike NNE and dip 25° to 30°E.

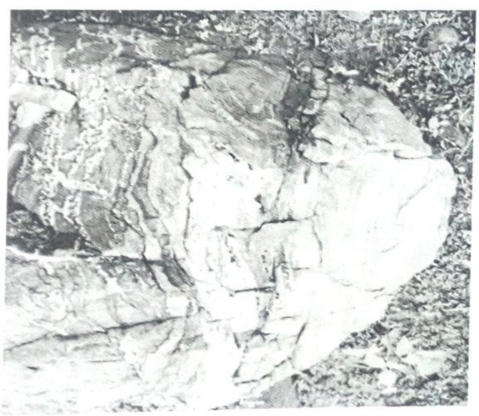

Figure 2.Migmatite outcrop (N9^{0}33' 50.8" and E6^{0}35'31")

Figure 3. Fractured Schist (N9^{0} 33'39.62" and E 6^{0} 35' 39.84")

Figure 4. Amphibolite (N9^{0} 33'20.16" and E 6^{0} 34' 59.66")

Figure 5. Fractured quarzite (N9^{0} 34'22.8" and E 6^{0} 35' 39.84")

Figure 6. Fractured Granite (N9^{0} 33'15.36" and E 6^{0} 34' 12")

Figure7 is the geological map produced from the spatial distribution of the outcrops.

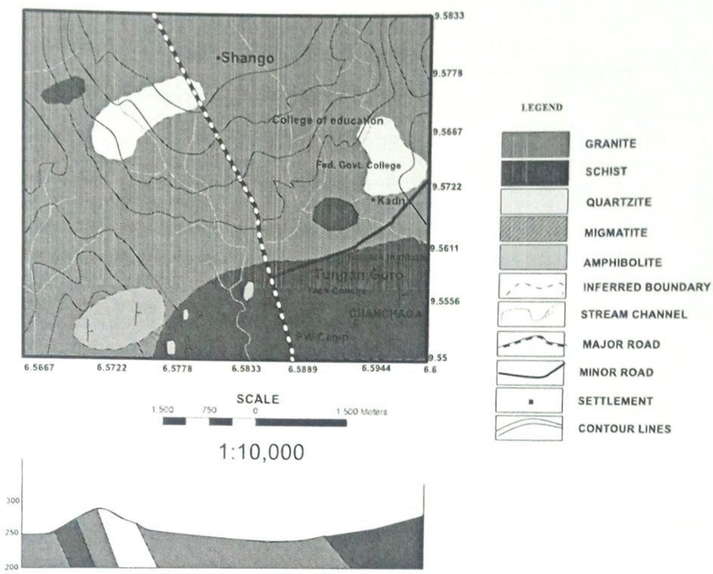

Figure 7. Geological map of Kadna

The map reveals that the granite intruded into the migmatite, schist and quartzite. The intrusive process must have generated the fractures in the outcrops. Rosette diagram plot of the joints is figure 8.

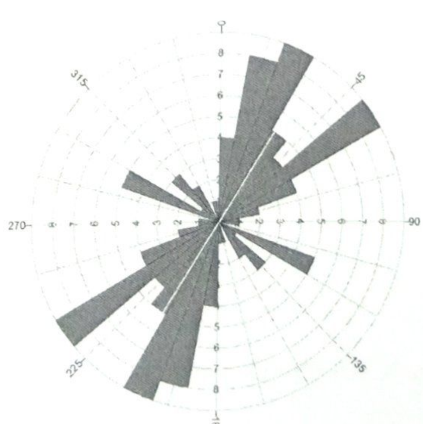

Figure 8: Rosette diagram plot of the measured joints

It reveals that the principal joint direction is NNE-SSW, which constitute the strike joints. A subsidiary joint direction is NW-SE, which can be described as dip joints. Figure 9 is the spatial location of the geoelectric measurement stations.

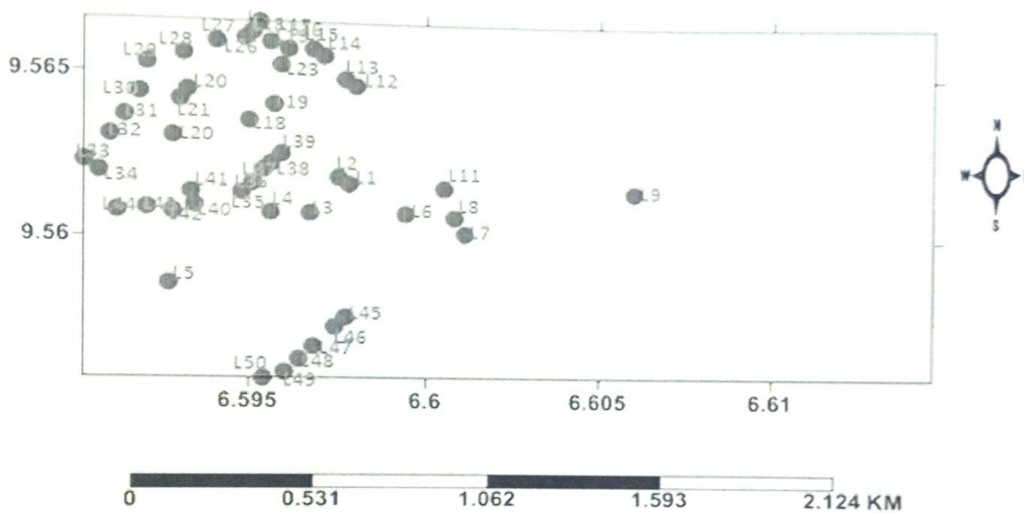

Figure 9. The geoelectric measurement stations

Some of the modeled resitivity sounding curves are figures 10, 11, 12 and 13. They are respectively HKH, KHKHKH, HKHKH and HKHK type curves.

Distance	Resistivity
1.00	222.7700
1.50	186.7100
2.00	96.8380
3.00	53.9650
5.00	45.8380
7.00	47.4220
10.00	54.1930
15.00	56.4970
20.00	72.2520
25.00	86.1570
30.00	124.4500
40.00	182.4200
50.00	221.1200
60.00	280.3700
70.00	338.1200
80.00	274.4500
100.00	539.8500

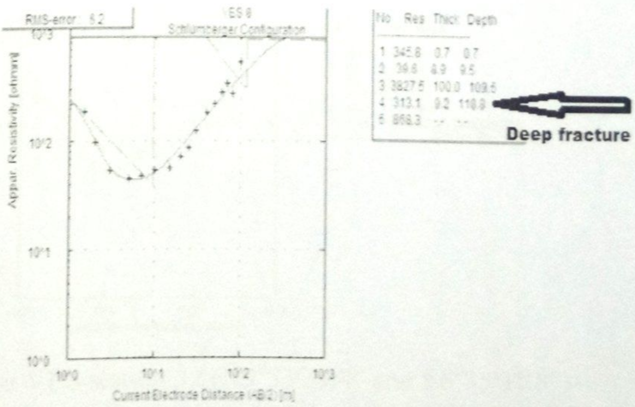

No	Res	Thick	Depth
1	345.6	0.7	0.7
2	39.6	8.9	9.5
3	3827.5	100.0	109.5
4	313.1	9.2	118.8
5	868.3	--	--

Figure 10. Deep fracture at VES station 8 (N9^{0}33'36.9" and E6^{0}36'4.0")

Distance	Resistivity
1.00	285.1400
1.50	394.9100
2.00	440.7300
3.00	533.2900
5.00	674.5800
7.00	673.8700
10.00	229.6500
15.00	334.8800
20.00	229.6500
25.00	197.1000
30.00	166.8150
40.00	135.8800
50.00	144.5900
60.00	161.8600
70.00	174.2300
80.00	51.9880
100.00	221.4000

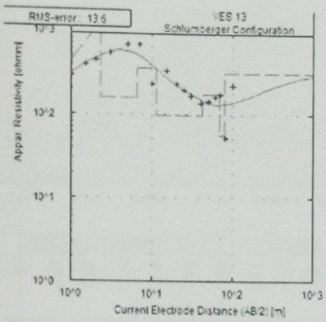

No	Res	Thick	Depth
1	205.2	0.6	0.6
2	1276.7	1.7	2.3
3	155.1	4.2	6.5
4	357.2	4.8	11.2
5	98.6	30.7	41.9
6	174.7	26.9	68.8
7	56.6	9.4	78.2
8	312.4	-.-	-.-

Deep fracture

Figure 11: Deep fracture at VES station 13 (N9^{0}33'56.3" and E6^{0}35'49.7")

Distance	Resistivity
1.00	479.7800
1.50	429.3300
2.00	318.8700
3.00	216.4800
5.00	76.7080
7.00	71.9610
10.00	88.8710
15.00	94.9790
20.00	133.1700
25.00	209.9600
30.00	281.9900
40.00	212.4900
50.00	402.6600
60.00	383.0600
70.00	282.0200
80.00	318.1200
100.00	543.8800

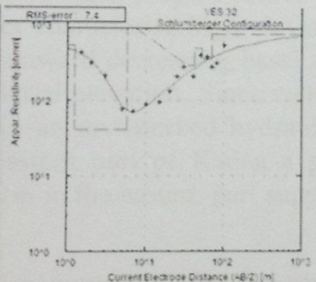

No	Res	Thick	Depth
1	531.9	1.2	1.2
2	40.7	4.6	5.8
3	1108.6	28.0	33.8
4	292.3	8.7	42.4
5	492.9	10.0	52.4
6	364.2	17.9	70.3
7	770.3	-.-	-.-

Deep fracture

Figure 12. Deep fracture at VES station 32 (N9^{0}33'47.2" and E6^{0}35'28.3")

Distance	Resistivity
1.00	252.8300
1.50	219.9500
2.00	204.8100
3.00	130.1300
5.00	62.4560
7.00	37.3020
10.00	27.2910
15.00	31.3410
20.00	41.7150
25.00	48.4380
30.00	47.3920
40.00	43.0850
50.00	44.0060
60.00	58.2340
70.00	68.2670
80.00	84.2710
100.00	77.4370

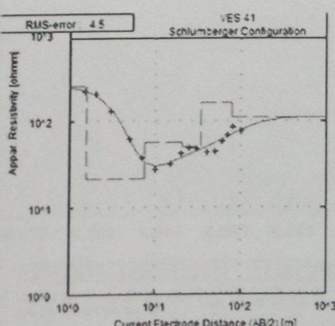

No	Res	Thick	Depth
1	256.3	1.6	1.6
2	21.7	5.9	7.4
3	56.3	13.2	20.6
4	49.4	13.1	33.7
5	160.5	44.3	78.0
6	109.5	-	

Deep fracture

Figure 13. Deep fracture at VES station 32 (N9^{0}33'39.4" and E6^{0}35'31.8")

The resistivity values are between 60 and 313Ωm at depth greater than 60m. Drilling results show that fractures characterised by such resistivity values are very often water filled within the northern Nigerian Massif. Figure 14 is the resistivity contour map for the deep fractures.

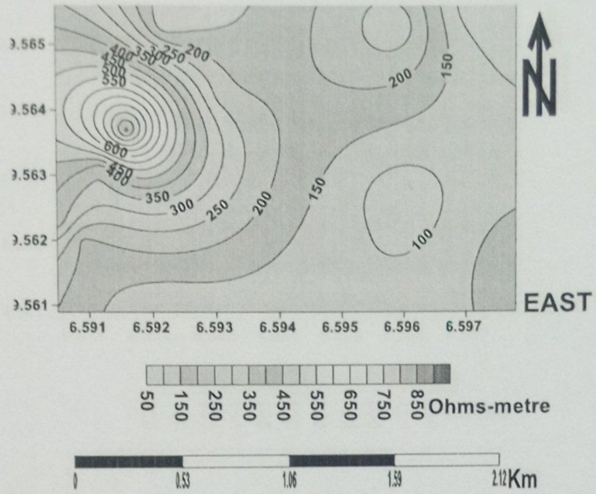

Figure 14. Resistivity contour map for deep fractures

It reveals that the resistivity generally decreases eastward and southeastward. Figures 15 and 16 are SP and fractures' basal elevation maps. Positive SP values characterise low elevation areas while negative SP values characterise high elevation areas. The maps show eastward increasing SP positivity and eastward decreasing basal elevation. The increasing positive SP trend conforms to decreasing basal elevation. Since water flow is gravity driven from higher elevation to lower elevation in an undisturbed hydraulic environment, groundwater would flow eastward. This makes eastern part of Kadna a groundwater convergence zone. The resistivity values of 100-200 Ωm in the eastern part supports inference of water occurrence in the fractures.

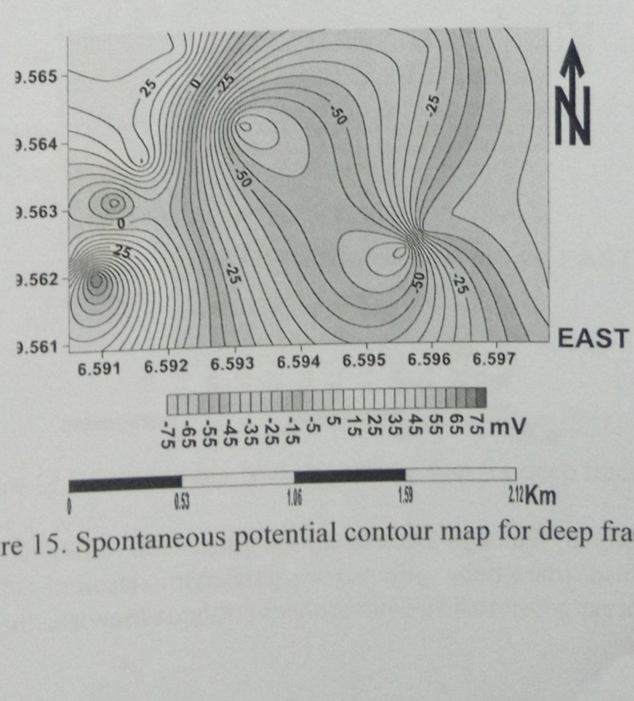

Figure 15. Spontaneous potential contour map for deep fractures

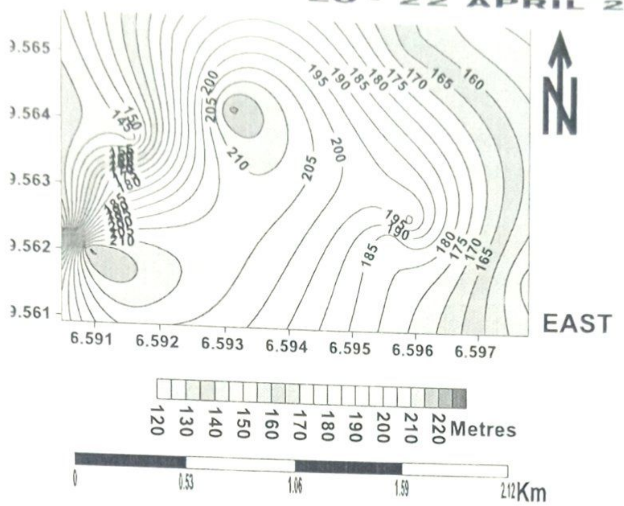

Figure 16. Basal elevation contour map for deep fractures

Figure 17 is the measured induced polarization contour map. Induced polarization effect characterizes regions of low permeability such as clay bodies. Such clayey regions are also characterised by low resistivity values. Induced polarization effect also characterizes bodies with disseminated ore minerals. But in disseminated ore bodies, such IP effects are associated with high resistivity values.

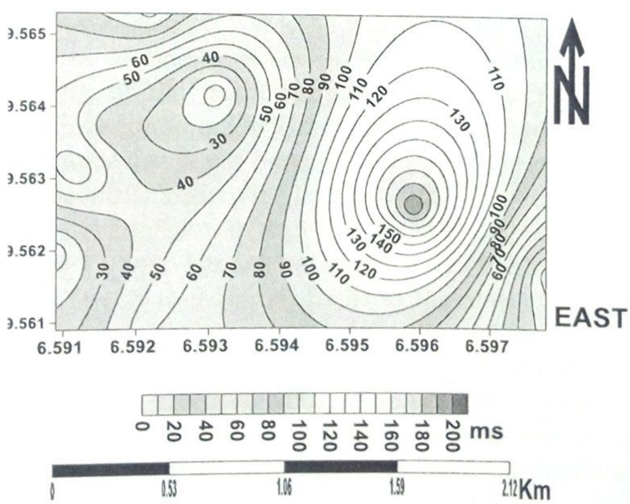

Figure 17. Induced polarisation contour map for deep fractures

The IP map reveals IP values decreasing southeastward, in rough parallelism with decreasing resistivity trend. This indicates increasing permeability southeastward. The slowly changing resistivity values southeastward supports the inference of increasing permeability in this direction. The IP values (40 to 100ms) and low resistivity values (100 to 200 Ωm) at depth deeper than 60m indicate water-filled fractures in the southeastern part of Kadna. Figures 18 is the thickness contour map for the deep fractures.

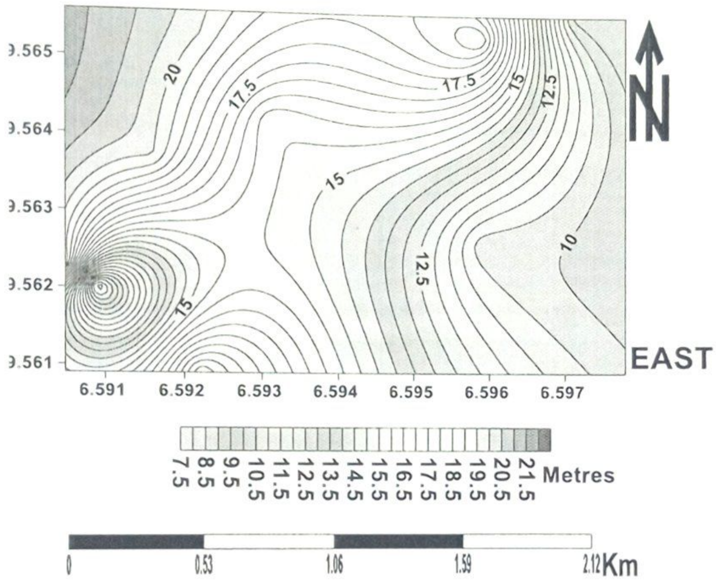

Figure 18: Thickness contour map for deep fractures

The fractures are between 10 and 13m thick in the southeast of Kadna. Shallow fractures with thickness less than 10m have been proved to be water bearing from drilling results in Kadna. This enhances the chances of finding water in the deep fractures. Figure 19 is a pictorial illustration of the ranking of the deep fracture areas for water borehole drilling. The easternmost area (within longitude 6.596°E to 6.610°E and latitude 9.561°N to 9.566°N) ranks first in order of choice for water borehole drilling. The attributes that chracterise the first ranking area are electrical resistivity between 100 and 200 Ωm, SP values between -30 and +15 mv, basal elevation lower than 180 m with respect to sea level, and fracture thickness between 10 and 13.5 m. The second ranking area lies within longitude 6.5945°E to 6.5965°E and latitude 9.561°N to 9.566°N. It shares the attributes of the first ranking area, except that the second ranking area has a basal elevation that is higher than 180m. The third ranking area lies within longitude 6.5945°E to 6.5965°E and latitude 9.561°N to 9.566°N. It differs from the second ranking area in having SP values more negative (for example, -35m, -40, -60 mv). The spatial locations of the drilling prospects are skewed NNE-SSW. This suggests that the NNE-SSW fractures (or strike joints) govern groundwater occurrence within the deep fractures.

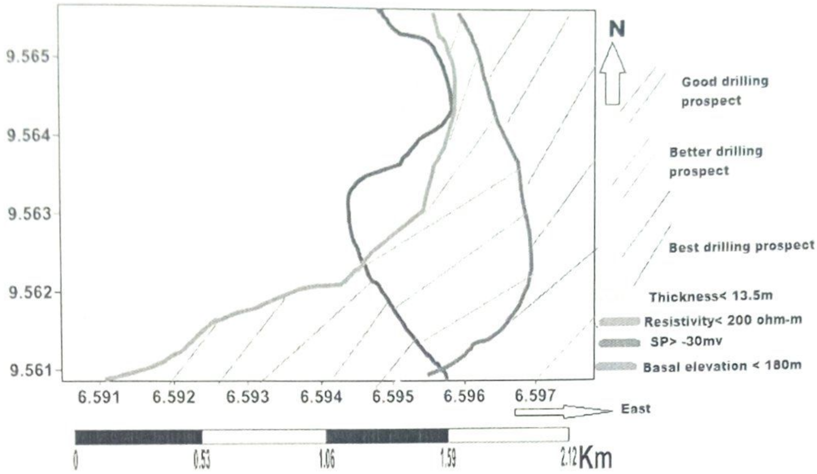

Figure 19. Thickness contour map for deep fractures

Results and Suggestions

Kadna is dotted with outcrops of migmatite, schist and amphibolites that strike NNE and dip 25-30°E, as well as outcrops of quartzite. All the outcropping lithologies are intruded by Older Granites. The resistivity sounding data reveals fractures at depths greater than 60m, which are called deep fractures. Iso-resistivity, SP and basal elevation maps reveal that groundwater convergence regions exist in the easternmost part of Kadna. The easternmost area within Longitude 6.596°E to 6.610°E and Latitude 9.561°N to 9.566°N contain deep fractures characterised by resistivity value of 100-200 Ωm, SP values of -30 to +50 mv and basal elevation lower than 180 m with respect to sea level. Their thickness is between 10 and 13.5 m, and are considered best drilling prospect within the deep fractures. Other drilling prospects lie within longitude 6.5945°E to 6.5965°E and latitude 9.561°N to 9.566°N, as well as longitude 6.5945°E to 6.5965°E and latitude 9.561°N to 9.566°N. Groundwater occurrence in the deep fractures appears to be controlled by the NNE-SSW (strike) fractures.

References

Ajibade, A.C., Anyanwu, N.P.C., Okoro, A.U., and Nwajide, C.S., 2008. The gelogy of Minna area: Explanation of 1:250,000 Sheet 42 (Minna). Nigerian Geological Survey Agency Bull. No. 84.

Ayuk, M.A., Adelusi, A.O. and Adiat, K.A.W., 2013. Evaluation of groundwater potential and aquifer protective capacity assessment at Tutugbua-Olugboyega area, off Ondo road, Akure, SW Nigeria, International Journal of Physical Sciences, 8(1): 37-50.

Dan Hassan, M.A. and Olorunfemi, M.O., 1999. Hydrogeophysical investigation of a basement terrain in the north central part of Kaduna State, Nigeria, Journal of Mining and Geology, 35(2): 189-206.

Ojo, A.O., Olorunfemi,M.O., 2013. A graphical and semi-quantitative technique for investigating vertical electrical sounding curves(VES) for indices of confined fractured basement column, Ife Journal of Science, 15(2): 353- 366.

Ojoina, 0.A., 2014. Hydrogeophysical investigation for groundwater in Lokoja metropolis, Kogi State, North Central Nigeria, Journal of Geography and Geology, 6 1(20): 81-95.

Olorunfemi, M.O., 2009. Groundwater exploration, borehole site selection and optimum drill depth in basement complex terrain. Water resources special publication series.

Oluyide, P.O., 1988. Structural trends in the Nigerian Basement Complex. In: Precambrian Geology of Nigeria, Geological Survey of Nigerian publication of the proceedings of the first symposium on the Precambrian Geology of Nigera, 93- 98.

Ratnakumari, Y., Rai, S.N, Thiagarajan, S. and Kumar, D., 2012. 2D Electrical resistivity imaging for delineation of deeper aquifers in a part of the Chandrabhaga river basin, Nagpur District, Maharashtra, India Current Science, 102(1): 61-69.

Tswako, M., Unuevho, C.I., Amadi, A.N., Ejepu, J.S., and Onuoha, K.M., 2017. Geoelectrical Prospecting for Regolith Aquifer in Kundu, Zungeru Sheet 163, Nigeria. Minna Journal of Geosciences,.1(1):149- 164.

Unuevho, **C.,** Onuoha, K.M., Ogunbajo, M.I., and Amadi, A.N., 2016. Hydrogeological and Geoelectrical Prospecting for Groundwater within parts of Northeastern Bosso, Minna, North-Central Nigeria region, Water Resources(Journal of the Nigerian Association of Hydrogeologists*)*, 26(1&2): 100-121.